HHS Public Access

Author manuscript

Biochim Biophys Acta. Author manuscript; available in PMC 2016 May 01.

Prostacyclin post-treatment improves LPS-induced acute lung injury and endothelial barrier recovery via Rap1

Anna A. Birukova[1], **Fanyong Meng**[1], **Yufeng Tian**[1], **Angelo Meliton**[1], **Nicolene Sarich**[1], **Lawrence A. Quilliam**[2], and **Konstantin G. Birukov**[1]

[1]Lung Injury Center, Section of Pulmonary and Critical Medicine, Department of Medicine, University of Chicago, Chicago, Illinois 60637, USA

[2]Department of Biochemistry and Molecular Biology, Indiana University School of Medicine, Indianapolis, IN 46202-5122, USA

Abstract

Protective effects of prostacyclin (PC) or its stable analog beraprost against agonist-induced lung vascular inflammation have been associated with elevation of intracellular cAMP and Rac GTPase signaling which inhibited the RhoA GTPase-dependent pathway of endothelial barrier dysfunction. This study investigated a distinct mechanism of PC-stimulated lung vascular endothelial (EC) barrier recovery and resolution of LPS-induced inflammation mediated by small GTPase Rap1. Efficient barrier recovery was observed in LPS-challenged pulmonary EC after prostacyslin administration even after 15 hrs of initial inflammatory insult and was accompanied by the significant attenuation of p38 MAP kinase and NFkB signaling and decreased production of IL-8 and soluble ICAM1. These effects were reproduced in cells post-treated with 8CPT, a small molecule activator of Rap1-specific nucleotide exchange factor Epac. By contrast, pharmacologic Epac inhibitor, Rap1 knockdown, or knockdown of cell junction-associated Rap1 effector afadin attenuated EC recovery caused by PC or 8CPT post-treatment. The key role of Rap1 in lung barrier restoration was further confirmed in the murine model of LPS-induced acute lung injury. Lung injury was monitored by measurements of bronchoalveolar lavage protein content, cell count, and Evans blue extravasation and live imaging of vascular leak over 6 days using a fluorescent tracer. The data showed significant acceleration of lung recovery by PC and 8CPT post-treatment, which was abrogated in Rap1a−/− mice. These results suggest that post-treatment with PC triggers the Epac/Rap1/afadin-dependent mechanism of endothelial barrier restoration and downregulation of p38MAPK and NFkB inflammatory cascades, altogether leading to accelerated lung recovery.

Corresponding address: Konstantin Birukov, MD, PhD Lung Injury Center Section of Pulmonary and Critical Medicine Department of Medicine University of Chicago 5841 S. Maryland Ave, Office N-611 Chicago, IL 60637 Phone: 773-834-2636 Fax: 773-834-2683 kbirukov@medicine.bsd.uchicago.edu.

Publisher's Disclaimer: This is a PDF file of an unedited manuscript that has been accepted for publication. As a service to our customers we are providing this early version of the manuscript. The manuscript will undergo copyediting, typesetting, and review of the resulting proof before it is published in its final citable form. Please note that during the production process errors may be discovered which could affect the content, and all legal disclaimers that apply to the journal pertain.

1. INTRODUCTION

Acute respiratory distress syndrome (ARDS) represents a spectrum of common syndromes in response to a variety of infectious and non-infectious insults. Until now there remain few effective therapeutic approaches towards for this devastating illness, mortality rates (30-40%) remain unacceptably high [1,2], and novel treatments aimed at reducing vascular leak and acute inflammation in lung injury have yet to be developed. Despite the recent progress towards understanding the basis of increased EC permeability (see [3,4] for review), molecular events stimulating EC barrier restoration in the course of ALI remain poorly understood.

Prostaglandins represent an important group of lipid mediators with barrier-protective potential towards the vascular endothelium [5]. While prostaglandin E2 (PGE$_2$) and thromboxanes appear to participate in the propagation of inflammation [6,7], other prostaglandins such as PGE$_1$ and prostacyclin (PC) exhibit potent protective effects in ischemia-reperfusion [8] and ventilator induced lung injury [9]. The beneficial effects of prostaglandins extend beyond their vasodilating effects and regulation of local circulation and involve direct protective effects on the vascular endothelium [5,10,11]. Protective effects of PC and its synthetic analogs, iloprost and beraprost, have been characterized by several groups [5,11-14].

Elevation of intracellular cyclic AMP (cAMP) levels is a major cellular response to PC. In pulmonary vascular endothelia, PC-induced elevation of cAMP at submembrane compartment promotes enhancement of the EC barrier [5,11,15]. Barrier-protective effects of cAMP-elevating agents on EC monolayers have been previously associated with an inhibitory role of cAMP-activated protein kinase A towards an agonist-induced EC contractile response mediated by RhoGTPase and myosin light chain kinase and leading to EC barrier disruption [16-19]. An alternate, PKA-independent pathway of EC barrier enhancement, involves cAMP-activated guanine nucleotide exchange factor (GEF) Epac1 and its target Rap1 GTPase, which strengthens the endothelial barrier by *de novo* formation or enhancing the existing intercellular adhesive complexes via its cell adhesion effector afadin [20,21].

It is also important to note that the intracellular location of cAMP pool critically determines its physiological outcome. While PC-induced generation of cyclic AMP in the subplasma membrane compartment activates PKA and Epac signaling leading to tightening of cell adhesions, strengthening of cortical actin cytoskeleton, reduction of actomyosin contraction, and enhancement of EC barrier described above, expansion of cAMP from sub-membrane compartment to the cytosolic compartment caused by soluble adenylate cyclases from pathogenic bacteria disrupts the endothelial barrier through PKA-mediated disassembly of microtubules [22,23].

Afadin is a scaffold protein activated by small GTPase Rap1, which promotes the assembly of cadherin-based adherens junctions [24,25], but also interacts with tight junction protein ZO-1 and adherens junction proteins α-catenin and p120-catenin. Rap1-induced p120-catenin association with afadin promotes p120-catenin localization to the adherens junctions and enhances AJ – TJ interactions in endothelial cells [26].

In addition, Rap1 activates Rac-specific guanine nucleotide exchange factors Tiam1 and Vav2 and promotes the parallel pathway of EC barrier by stimulating Rac GTPase signaling [11,27]. In contrast to the well recognized role of Rac1 signaling in endothelial barrier enhancement and the negative Rac-Rho crosstalk mechanism of EC barrier protection in the models of agonist-induced permeability, a role of Rap1 signaling in EC barrier restoration during septic inflammation and the link between cytoskeletal remodeling and modulation of inflammatory signaling in EC remains completely unexplored.

Many experimental models for screening novel protective compounds utilize preventive or concurrent treatment during ALI induction, while post-treatment remains the more clinically relevant intervention. These differences in application of protective agonists may have a dramatic impact on the outcome and interpretation of molecular mechanisms contributing to the downregulation or resolution of ongoing injury in contrast to preventing the initial disruptive signaling leading to ALI.

In this study we used biochemical, molecular, and functional approaches to characterize effects of PC post-treatment on the *in vitro* and *in vivo* models of LPS-induced lung injury. Using pharmacologic inhibitors and activators of Epac, genetic model of Rap1a knockout mice and Rap1 knockdown *in vitro*, we investigated a role of Epac-Rap1 mechanism in the modulation of LPS-induced ALI by PC post-treatment.

2. MATERIALS AND METHODS

2.1. Cell culture and reagents

Human pulmonary artery endothelial cells (HPAEC) and cell culture medium were obtained from Lonza Inc (Allendale, NJ), and used at passages 5-8. Unless specified, biochemical reagents were obtained from Sigma (St. Louis, MO). PC and beraprost were obtained from Cayman (Ann Arbor, MI); 8-(4-Chlorophenylthio)-2′-O-methyl-adenosine-3′,5′-cyclic monophosphate (8CPT) and Epac cell permeable inhibitor ESI-09 were purchased from Calbiochem (La Jolla, CA). Phospho-p38, IκBα, NFκB, β-actin antibodies were obtained from Cell Signaling (Beverly, MA); Rap1, phospho-VE-cadherin, VE-cadherin, ICAM1, and VCAM1 from Santa Cruz Biotechnology (Santa Cruz, CA). All reagents for immunofluorescence were purchased from Molecular Probes (Eugene, OR).

2.2. Measurement of endothelial permeability

The cellular barrier properties were analyzed by measurements of transendothelial electrical resistance (TER) across confluent human pulmonary artery endothelial monolayers using an electrical cell-substrate impedance sensing system (Applied Biophysics, Troy, NY) as previously described [28,29].

2.3. Neutrophil migration and adhesion assays

Neutrophil chemotaxis was measured in a 96-well chemotaxis chamber (Neuroprobe, Gaithersburg, MD) as described previously [30]. Briefly, freshly isolated neutrophils were placed in a 96-well chemotaxis chamber and incubated with 200 μl of preconditioned culture media, which was collected from stimulated EC cultures. Preliminary experiments have established that the number of cells (4×10^4 cells) used allow the optimal cell migration without clogging the pores of transwell filter of the upper chamber. Data were expressed as percent of cell migration. PMN adhesion to the EC was assessed by adding the neutrophils freshly isolated from healthy donors to the EC monolayers grown in the 6-well plates. Neutrophil adhesion on HPAEC was assessed as described previously [31]. Neutrophil adhesion data were expressed as percentage of adhesion for all treated groups.

2.4. siRNA transfection

To reduce the content of endogenous Rap1 or afadin, cells were treated with gene-specific siRNA duplexes [26,32]. Pre-designed standard purity siRNA sets (*Homo sapiens*) were ordered from Dharmacon (Lafayette, CO), and transfection of EC with siRNA was performed as previously described [33]. After 48-72 hrs of transfection, cells were used for experiments or harvested for western blot verification of specific protein depletion. Nonspecific, non-targeting siRNA (Dharmacon, Lafayette, CO) was used as a control treatment.

2.5. Immunofluorescence

Endothelial monolayers plated on glass cover slips were subjected to immunofluorescence staining as described previously [34]. Slides were analyzed using a Nikon video imaging system (Nikon Instech Co., Tokyo, Japan). Images were processed with Image J software (National Institute of Health, Washington, USA) and Adobe Photoshop 7.0 (Adobe Systems, San Jose, CA) software. Quantitative analysis of paracellular gap formation was performed as previously described [29,35,36]. The 16-bit images were analyzed using MetaVue 4.6 software (Universal Imaging, Downington, PA). The gap formation was expressed as a ratio of the gap area to the area of the whole image. The values were statistically processed using Sigma Plot 7.1 (SPSS Science, Chicago, IL) software. For each experimental condition at least 10 microscopic fields in each independent experiment were analyzed.

2.6. Differential protein fractionation and immunoblotting

Confluent HPAEC were stimulated with LPS with or without PC and nuclear fraction was isolated using S-PEK kit (EMD Chemicals, Gibbstown, NJ). Immunoblotting detection of proteins of interest was performed as described previously [37]. Protein extracts from mouse lungs or EC were separated by SDS-PAGE, transferred to polyvinylidene difluoride membranes, and the membranes were incubated with specific antibodies of interest. Equal protein loading was verified by probing for β-actin. Immunoreactive proteins were detected with the enhanced chemiluminescent detection system according to the manufacturer's protocol (Amersham, Little Chalfont, UK).

2.7. Measurement of cytokines and chemokines

The concentrations of KC in mouse bronchoalveolar lavage (BAL) fluid samples were measured using a Mouse Cytokine Multiplex Panel according to the manufacturer's protocol (Millipore, Billerica, MA). For interleukin-8 (IL-8) and soluble ICAM1 (sICAM1) measurements in preconditioned medium of human pulmonary EC cultures, supernatants from treated EC were collected and centrifuged to remove debris. IL-8 and sICAM1 levels were determined by ELISA (R&D Systems, Minneapolis, MN) following manufacturer's protocol. Absorbance was read at 450 nm within 30 min in microplate reader (Thermomax; Molecular Devices, Menlo Park, CA).

2.8. Animal studies

All animal care and treatment procedures were approved by the University of Chicago Institutional Animal Care and Use Committee. Animals were handled according to the National Institutes of Health Guide for the Care and Use of Laboratory Animals. *Rap1a−/−* mice have been described elsewhere [38,39]. C57BL/6J mice were purchased from Jackson Laboratories (Bar Harbor, ME). Bacterial lipopolysaccharide (LPS, 0.63 mg/kg body wt; *Escherichia coli* O55:B5) or sterile water was injected intratracheally in a small volume (20–30 μl) using a 20-gauge catheter (Exelint International, Los Angeles, CA). Beraprost (20 μg/kg), 8CPT (20 μM/kg) or sterile saline solution was administrated 5 hrs after LPS instillation by intravenous injection in the external jugular vein. These doses have been selected based on results of pilot studies, which showed potent anti-inflammatory and barrier protective effects of PC and 8CPT without visible adverse effects on experimental animals. After 18 hours of LPS challenge, animals were sacrificed by exsanguination under anesthesia. BAL was performed using 1 ml of sterile Hanks balanced salt buffer and measurements of cell count and protein concentration were conducted as previously described [40]. For analysis of LPS-induced lung vascular leak, Evans blue dye (30 ml/kg) was injected into the external jugular vein 2 hrs before termination of the experiment. Measurement of Evans blue accumulation in the lung tissue was performed by spectrofluorimetric analysis of lung tissue lysates according to the protocol described previously [41,42]. For histological assessment of lung injury, the lungs were harvested without lavage collection and fixed in 10% formaldehyde. After fixation, the lungs were embedded in paraffin, cut into 5-μm sections, and stained with hematoxylin and eosin. Sections were evaluated at 40x magnification.

2.9. *In vivo* optical imaging

Mice were injected with 100 μl of 2 nmol Angiosense 680 EX (a vascular fluorescent blood pool imaging agent purchased from PerkinElmer, Inc., Boston, MA; cat# NEV10054EX), intravenously via tail vein. After 24 hours, fluorescent optical imaging was performed in the Integrated Small Animal Imaging Research Resource (iSAIRR) at the University of Chicago using Xenogen IVIS 200 Spectrum (Caliper Life Sciences. Alameda, CA). Mice were exposed to isoflurane anesthesia with O_2 through the gas anesthesia manifold and placed on the imaging stage. Acquisition and image analysis were performed with Living Image 4.3.1 Software.

2.10. Statistical analysis

Results are expressed as means ±SD of three to eight independent experiments. Stimulated samples were compared to controls by unpaired Student's t-test. For multiple-group comparisons, one-way ANOVA and Tukey's post hoc multiple-comparison test were used. $P < 0.05$ was considered statistically significant.

3. RESULTS

3.1. Effects of PC post-treatment on LPS-induced endothelial hyperpermeability and disruption of monolayer integrity

Treatment of ongoing inflammation with protective compounds represents a more clinically relevant scenario of pharmacological intervention. Therefore, in the following studies we evaluated the effects of PC post-treatment in the model of EC barrier dysfunction and inflammation induced by LPS. PC added after 30 min, 2 hrs, 5 hrs or 15 hrs of LPS stimulation exhibited potent barrier protective effects reflected by pronounced and sustained elevation of transendothelial electrical resistance (TER) (Figure 1A).

Because previous studies by our group described a role for small GTPase Rap1 activated by Rap1-specific guanine nucleotide exchange factor Epac in the direct effect of PC on EC barrier [11], we examined a role of the Epac-Rap1 pathway in barrier recovery of LPS-challenged EC monolayers. In these experiments, LPS-challenged EC were treated with selective Epac activator, 8CPT, and the EC permeability response was monitored by measurements of TER. Post-treatment with 8CPT 30 min - 15 hrs after LPS challenge caused recovery of EC barrier (Figure 1B).

Recovery of LPS-induced EC barrier failure by PC post-treatment monitored by TER measurements was further linked to cytoskeletal changes. EC stimulation with LPS for 5 hrs caused the formation of actin stress fibers (Figure 1C), disruption of the continuous line of VE-cadherin positive paracellular adherens junctions (Figure 1D) and the appearance of paracellular gaps reflecting compromised EC barrier. Remarkably, the addition of PC after 5 hrs of LPS treatment caused reduction of stress fibers and restoration of the continuous adherens junction pattern accompanied by the resealing of paracellular gaps observed 30 min – 2 hrs after PC or 8CPT post-tretament (Figure 1CD). The bar graph represents results of quantitative analysis of PC and 8CPT post-treatment effects on LPS-induced gap formation.

3.2. PC post-treatment suppresses LPS-induced EC inflammatory activation

We investigated the effects of PC and 8CPT post-treatment on LPS-induced activation of inflammatory signaling. EC exposure to LPS for 2.5 hrs caused pronounced phosphorylation/activation of p38 MAP kinase, degradation of the IκBα inhibitory subunit (Figure 2A), and nuclear translocation of NFκB (Figure 2B) required for inflammatory gene expression. These effects were suppressed by post-treatment with PC or 8CPT 30 min after LPS challenge.

At later time points (24 hrs), LPS increased expression of ICAM1 and VCAM1, the adhesion molecules involved in EC-neutrophil interaction, while post-treatment with PC 5 hrs after LPS challenge abolished these effects (Figure 2C). Similar effects were observed in experiments with 8CPT post-treatment.

In complementary studies we measured the production of soluble ICAM1 (sICAM1) and neutrophil chemoattractant cytokine IL-8. The addition of PC 5 hrs after LPS challenge markedly attenuated sICAM1 and IL-8 production by pulmonary EC detected in the preconditioned culture medium 24 hrs after LPS addition (Figure 2D). Similar effects were observed in cells post-treated with 8CPT.

Activation of the vascular endothelium by inflammatory agents stimulates neutrophil adhesion to the EC lining the vascular luminal surface and following neutrophil transmigration through the EC monolayer leading to neutrophil recruitment to the inflamed lung parenchyma. Effects of PC post-treatment of LPS-induced lung dysfunction were evaluated in cell functional assays. Exposure of pulmonary EC to LPS (24 hrs) stimulated neutrophil migration and adhesion. Importantly, neutrophil migration stimulated by preconditioned medium from LPS-stimulated EC (Figure 2E) and EC-neutrophil interactions (Figure 2F) were significantly attenuated by post-treatment with PC or 8CPT 5 hrs after LPS addition.

3.3. Rap1 pathway is involved in EC recovery upon PC post-treatment

Our recent study demonstrated a role of Rap1 signaling during EC barrier restoration after thrombin-induced increase in EC permeability [32]. The following experiments tested involvement of the Rap1 mechanism in suppression of inflammatory signaling and barrier restoration in LPS-challenged pulmonary EC caused by PC post-treatment.

Inhibition of PC-induced Rap1 activation was first achieved by cell pretreatment with the Epac1 inhibitor, which blocked PC-induced activation of the Epac1-Rap1 pathway. Such inhibition of Epac1-Rap1 abolished the anti-inflammatory effect by PC reflected by attenuation of LPS-induced IkBa degradation (Figure 3A) and ICAM1 and VCAM1 expression (Figure 3B). EC incubation with Epac1 inhibitor did not significantly affect LPS-induced degradation of IkBa inhibitory subunit and increase in ICAM1 and VCAM1 expression. Inhibition of Epac1 also prevented the restoration of the EC barrier caused by PC post-treatment of LPS-challenged EC (Figure 3C).

The role of Rap1 in EC barrier restoration induced by PC post-treatment was further assessed in experiments with siRNA-mediated Rap1 knockdown. Increased VE-cadherin peripheral staining caused by PC post-treatment (1 hr after LPS), which reflects restoration of cell-cell adhesions in LPS-treated cells (Figure 4A, **left panel**) was attenuated in Rap1-depleted lung EC monolayers, which also exhibited increased paracellular gap formation. (Figure 4A, **right panel, shown by arrows**).

VE-cadherin phosphorylation at Y^{731} is known to promote disassembly of the adherens junction complexes [43,44]. Post-treatment with PC or 8CPT (5 hrs after LPS) attenuated LPS-induced VE-cadherin phosphorylation at Y^{731}, and also blocked expression of ICAM1

and VCAM1 (Figure 4B). Rap1 knockdown by gene-specific siRNA abolished the protective effects of PC and 8CPT post-treatment.

The role of the Rap1 pathway in the mediation of PC anti-inflammatory response was further investigated in experiments with inhibition of Rap1 cytoskeletal target afadin, involved in formation of cell-cell adhesive complexes [45,46]. siRNA-induced knockdown of afadin blocked the protective effects of PC post-treatment against LPS-induced disruption of VE-cadherin positive adherens junctions (Figure 5A) and inflammatory signaling monitored by increased ICAM1 expression (Figure 5B). These data suggest the key role of the Rap1-afadin axis in the mediation of PC effects on EC barrier restoration after an inflammatory insult. A role of the PC-Rap1 axis in tissue barrier restoration after inflammatory challenge was further evaluated in animal models.

3.4. Time course image analysis of PC post-treatment effects on lung recovery after LPS-induced injury

Lung vascular leak in mice treated with LPS and the stable PC analog beraprost was monitored in the same animals prospectively, 1, 2, 3, and 6 days after treatment. Angiosense 680 EX tracer was injected intravenously, and tracer accumulation in the lungs reflecting lung vascular barrier dysfunction and lung injury was performed in anesthetized animals using the non-invasive fluorescence optical imaging approach described in Methods. Accumulation of the fluorescent tracer reflecting lung inflammation and vascular barrier compromise was observed 24 hrs after LPS injection, reaching maximal levels at day 2 and gradually declining by day 6 (Figure 6A). Importantly, lung dysfunction was noticeably reduced in mice post-treated with beraprost 5 hrs after LPS challenge, and recovery of lung function occurred earlier than in mice without PC post-treatment. The results were supported by quantitative analysis of lung imaging data.

Results of live imaging studies were supported by conventional analysis of bronchalveolar lavage protein content and cell counts in parallel experiments. Intravenous injections of PC or 8CPT after 5 hours of LPS instillation significantly decreased BAL protein content and total cell count, in the LPS-treated mice (Figure 6B).

3.5. PC post-treatment effectively suppresses LPS-induced lung barrier dysfunction and inflammation *in vivo*

Effects of PC post-treatment on the lung vascular leak induced by LPS were further evaluated by measurements of Evans blue extravasation into the lung tissue. Administration of beraprost significantly reduced LPS-induced Evans blue accumulation in the lung parenchyma (Figure 7AB). In agreement with cell culture studies, beraprost post-treatment inhibited LPS-induced ICAM1 expression (Figure 7C) in the lung detected by western blot analysis of lung tissue homogenates.

3.6. Rap1 mediates improved recovery of LPS-induced lung injury caused by PC post-treatment

Although the Rap1b genetic variant of the Rap1 protein is expressed in vascular endothelium at higher levels [47], the vascular endothelial barrier function is more sensitive

to depletion of the Rap1a variant [48,49]. The role of Rap1 in the lung recovery after inflammatory insult was evaluated using the genetic model of *Rap1a−/−* mice. First, we evaluated the magnitude of LPS-induced lung injury in *Rap1a−/−* mice. Parameters of lung injury in *Rap1a−/−* mice and matching controls were analyzed at day 1, 2, 3, 5, and 7 after LPS administration. In comparison to wild type controls, *Rap1a−/−* mice developed more severe lung injury in response to LPS which was reflected by measurements of protein content (Figure 8A) and cell counts (Figure 8B) in BAL samples from LPS-challenged wild type and knockout animals. Western blot analysis of lung tissue samples revealed more prominent ICAM1 expression in *Rap1a−/−* mice at day 5 after LPS challenge (Figure 8C).

The next experiments evaluated the effects of beraprost post-treatment in LPS-challenged control and Rap1a knockout animals. *Rap1a−/−* mice and matching controls were injected with vehicle or beraprost 5 hrs after the LPS challenge. Protective effects of PC post-treatment against LPS-induced increases in BAL cell count and protein content observed in wild type controls were abolished in *Rap1a−/−* mice (Figure 9A).

Histological analysis of lung tissue sections stained with hematoxylin and eosin showed that in contrast to wild type controls, the protective effects of PC against LPS-induced alveolar wall thickening and increased leukocyte infiltration were diminished in the Rap1 knockout mice (Figure 9B). Attenuation of LPS-induced ICAM1 expression by beraprost was observed in wild type controls and was abolished in *Rap1a−/−* mice (Figure 9C). Next, effects of PC on LPS-induced cytokine production were tested in control and *Rap1a−/−* mice. In consistence with *in vitro* results, protective effect of beraprost against LPS-induced elevation of mouse IL-8 homologue KC was suppressed in the Rap1 knockout animals (Figure 9D). Taken together, these results demonstrate pronounced anti-inflammatory and barrier-protective effects of PC post-treatment in the animal model of LPS-induced lung inflammatory injury and vascular leak and emphasize a key role of Rap1 in the mediation of PC protective effects.

4. DISCUSSION

The main finding of this study is a role of Rap1 signaling in attenuation of ongoing lung inflammation and barrier dysfunction in a septic model of ALI. This is also the first demonstration of a dramatic improvement of EC barrier function and ongoing lung injury achieved by post-treatment with PC and its stable analogs.

Many models of post-treatment show a relatively short efficient therapeutic window (10-30 min of post-treatment) effective to inactivate an injurious stimulus [50-52]. The PC pretreatment used in this study efficiently attenuated parameters of lung inflammation and accelerated EC barrier recovery even when it was administered 15 hrs after LPS challenge *in vitro* and 5 hrs after LPS challenge *in vivo*. In addition to analysis of BAL parameters of lung injury, we monitored the time course of lung vascular leak in control and PC-treated mice with LPS-induced ALI using a non-invasive live imaging approach. Live imaging of LPS-induced ALI in mice with or without PC post-treatment has been performed for the first time and demonstrated a significant acceleration of lung recovery by PC post-treatment. Tracking the time dependent changes in the same animal in the course of ALI is a powerful

approach aimed to diminish individual variability in the magnitude of inflammatory response to an intervention. This analysis was complemented by morphological and biochemical data and demonstrated high consistence of traditional parameters of ALI and live imaging data.

PC post-treatment caused remarkably rapid and potent recovery of barrier function in LPS-challenged EC. Importantly, the recovery effect of PC was reproduced by cell pretreatment with a specific activator of Epac-Rap1 signaling, 8CPT. The time course of EC barrier recovery suggests Rap1-induced activation on vascular EC cytoskeleton and restoration of the cell junction barrier as a leading mechanism of EC barrier recovery caused by PC post-treatment. Besides direct stimulation of cell junction assembly, Rap1 also promoted re-sealing of intercellular gaps in EC monolayers stimulated with thrombin [32]. These Rap1 effects had been associated with Rap1-dependent downregulation of Rho signaling via Rap1-induced Rac1-RhoA negative crosstalk. Rap1 activation in thrombin-treated pulmonary EC represented the mechanism of endothelial barrier auto-recovery and was mediated by the Rap1-specific guanine nucleotide exchange factor C3G stimulated by thrombin-activated Src kinase [32]. The rapid EC barrier recovery observed in this study suggests activation of similar mechanisms in a distinct model of EC barrier dysfunction caused by bacterial pathogens.

In addition to the rapid barrier recovery driven by cytoskeletal and cell junction remodeling, Rap1 activation by PC and 8CPT also blocked the LPS-induced inflammatory response. After binding to a LPS ligand, TLR4 sequentially recruits the adaptor molecules MyD88, IL-1R-associated kinase (IRAK), and TNF receptor-associated factor 6 (TRAF6). These adaptor molecules then activate MAP kinases JNK, p38, ERK1/2 and IκB, a cytoplasmic inhibitor of NFκB [53]. NFκB and MAP kinases mediate the LPS-induced production of proinflammatory cytokines. However, besides the canonical activation by the TLR4-MyD88-IRAK-TRAF6 cascade, the p38 MAPK and NFκB activity is positively regulated by the small GTPase, RhoA [54,55]. In turn, inhibition of the Rho pathway attenuated the inflammatory and barrier disruptive EC response to bacterial pathogens [56-60]. Rap1-mediated attenuation of Rho signaling described above in the model of thrombin-induced EC permeability [32], as well as downregulation of Rho-dependent lung injury by Rap1 activity in the animal model of ventilator-induced vascular leak [14] suggest a potential mechanism of ALI attenuation by Rap1-Rho negative crosstalk.

This study also shows attenuation of LPS-induced ICAM1 expression by the Epac-Rap1 mechanism. ICAM-1 is essential for stable adhesion and transmigration of leukocytes in most types of inflammatory processes. Blocking antibodies against ICAM-1 inhibit leukocyte adhesion, while the deletion of the cytoplasmic domain of ICAM-1 completely blocks neutrophil transmigration but not the adhesion, demonstrating the importance of ICAM-1–dependent signaling in mediating neutrophil transmigration [61]. Engagement of ICAM-1 by leukocytes results in tyrosine phosphorylation of VE-cadherin, which is required for efficient neutrophil TEM. Interestingly, ICAM-1 engagement leads to phosphorylation of VE-cadherin on tyrosines 658 and 731, which correspond to the p120-catenin and β-catenin binding sites, respectively. Such VE-cadherin phosphorylation may be mediated by tyrosine kinases, Src and Pyk2 [62], or by a RhoA-dependent mechanism [63]

and promotes disassembly of the VE-cadherin-catenin complex and internalization of VE-cadherin and p120-catenin leading to disassembly of adherens junctions and EC barrier compromise. LPS-induced disruption of adherens junctions associated with tyrosine phosphorylation of VE-cadherin was also observed in the current study. One consequence of AJ disassembly is EC barrier compromise leading to an influx of solutes and increased neutrophil infiltration into the lung, the process that perpetuates ongoing ALI.

Another consequence of AJ disassembly is the release of p120-catenin from cell junctions. In the context of LPS-induced lung inflammation, p120-catenin displacement from AJ and degradation may propagate inflammatory signaling. Molecular inhibition of p120-catenin has been associated with development of skin inflammation in p120-catenin knockout mice due to dysregulation of Rho signaling at cell-cell junctions [64]. Downregulation of p120-catenin in lung EC increased the inflammatory response of LPS and the mortality in the animal LPS-induced sepsis model [65]. These effects were associated with p120-catenin modulation of lung immune function by interfering with the association of TLR4 with its adaptor MyD88 to block TLR4 signaling and NFκB activation in endothelial cells.

Our data show that pharmacologic inhibition of Epac, Rap1 knockdown in pulmonary EC, or Rap1a knockout in mice exacerbated LPS-induced lung injury. Interestingly, protective effects of PC and 8CPT against LPS-induced adherens junction disassembly, EC barrier disruption and ICAM1 expression were attenuated by the knockdown of Rap1 effector afadin. Afadin involvement in regulating the expression of inflammatory molecules is a novel finding. How may afadin be possibly involved in Rap1 anti-inflammatory signaling? Afadin mediates the formation of nascent adherens junctions and directly interacts with cadherin-associated signaling protein p120-catenin [66]. Barrier enhancing signals stimulate afadin interaction with AJ and TJ protein partners. p120-catenin and ZO-1 [25,26], which leads to the strengthening of cell-cell junctions and enhancement of EC barrier integrity. Based on the previous reports and current data, we suggest that, as a Rap1 effector and adaptor protein, afadin preserves p120-catenin localization at adhesive complexes in PC-stimulated cells thus preventing p120-catenin from degradation and initiation of the TLR4-MyD88-NFκB inflammatory cascade described above. These data suggest a novel role for Rap1 signaling in the modulation of the EC innate immune response to bacterial pathogens via a Rap1-afadin-dependent mechanism.

In conclusion, this is the first study demonstrating the anti-inflammatory effects of Rap1-afadin axis in the models of LPS-induced lung injury. This study proposes a novel paradigm of dual Rap1-afadin-mediated anti-inflammatory mechanisms in ALI, which include: a) re-sealing of intercellular junctions leading to enhanced EC barrier and reduced transfer of inflammatory molecules to the lung parenchyma; and b) inhibition of EC inflammatory activation (manifested by activation of cell adhesion molecules and cytokine expression). Beneficial effects of specific activators of Rap1 signaling on ALI recovery may have a substantial impact on the drug design strategies leading to the generation of more effective or tissue-specific Rap1 activators. As vascular barrier-protective and anti-inflammatory therapeutic benefits of PC are currently offset by hypotensive side effects, the potential utilization of Epac and Rap1 activators may overcome the disadvantages of currently available PC analogs. In the future, attempts to develop efficient small molecule Rap1

activators may provide a novel aspect of treatment of ARDS and other conditions associated with inflammation and vascular barrier dysfunction.

AKNOWLEDGEMENTS

Non-standard Abbreviations

ALI	acute lung injury
BAL	bronchoalveolar lavage fluid
EC	endothelial cells
ECIS	electrical cell-substrate impedance sensing system
HPAEC	human pulmonary artery endothelial cells
LPS	lipopolysaccharide
MPO	myeloperoxidase
nsRNA	non-specific RNA
PC	prostacyclin
TER	transendothelial electrical resistance
XPerT	express permeability testing assay
8CPT	8-(4-Chlorophenylthio)-2′-O-methyl-adenosine-3′,5′-cyclic monophosphate

REFERENCES

1. Rubenfeld GD, Caldwell E, Peabody E, et al. Incidence and outcomes of acute lung injury. N Engl J Med. 2005; 353:1685–93. [PubMed: 16236739]

2. Ware LB, Matthay MA. The acute respiratory distress syndrome. N Engl J Med. 2000; 342:1334–49. [PubMed: 10793167]

3. Mehta D, Malik AB. Signaling mechanisms regulating endothelial permeability. Physiol Rev. 2006; 86:279–367. [PubMed: 16371600]

4. Birukov KG, Zebda N, Birukova AA. Barrier enhancing signals in pulmonary edema. Comprehensive Physiology. 2013; 3:429–84. [PubMed: 23720293]

5. Fukuhara S, Sakurai A, Sano H, et al. Cyclic AMP potentiates vascular endothelial cadherin-mediated cell-cell contact to enhance endothelial barrier function through an Epac-Rap1 signaling pathway. Mol Cell Biol. 2005; 25:136–46. [PubMed: 15601837]

6. Goggel R, Hoffman S, Nusing R, et al. Platelet-activating factor-induced pulmonary edema is partly mediated by prostaglandin E(2), E-prostanoid 3-receptors, and potassium channels. Am J Respir Crit Care Med. 2002; 166:657–62. [PubMed: 12204861]

7. Park GY, Christman JW. Involvement of cyclooxygenase-2 and prostaglandins in the molecular pathogenesis of inflammatory lung diseases. Am J Physiol Lung Cell Mol Physiol. 2006; 290:L797–805. [PubMed: 16603593]

8. Schutte H, Lockinger A, Seeger W, et al. Aerosolized PGE1, PGI2 and nitroprusside protect against vascular leakage in lung ischaemia-reperfusion. Eur Respir J. 2001; 18:15–22. [PubMed: 11510786]

9. Birukova AA, Fu P, Xing J, et al. Lung endothelial barrier protection by iloprost in the 2-hit models of ventilator-induced lung injury (VILI) involves inhibition of Rho signaling. Transl Res. 2010; 155:44–54. [PubMed: 20004361]

10. Baumer Y, Drenckhahn D, Waschke J. cAMP induced Rac 1-mediated cytoskeletal reorganization in microvascular endothelium. Histochem Cell Biol. 2008; 129:765–78. [PubMed: 18392843]

11. Birukova AA, Zagranichnaya T, Alekseeva E, et al. Prostaglandins PGE2 and PGI2 promote endothelial barrier enhancement via PKA- and Epac1/Rap1-dependent Rac activation. Exp Cell Res. 2007; 313:2504–20. [PubMed: 17493609]

12. Farmer PJ, Bernier SG, Lepage A, et al. Permeability of endothelial monolayers to albumin is increased by bradykinin and inhibited by prostaglandins. Am J Physiol Lung Cell Mol Physiol. 2001; 280:L732–8. [PubMed: 11238014]

13. Langeler EG, van Hinsbergh VW. Norepinephrine and iloprost improve barrier function of human endothelial cell monolayers: role of cAMP. Am J Physiol. 1991; 260:C1052–9. [PubMed: 1709785]

14. Birukova AA, Fu P, Xing J, et al. Rap1 mediates protective effects of iloprost against ventilator induced lung injury. J Appl Physiol. 2009; 107:1900–10. [PubMed: 19850733]

15. Cullere X, Shaw SK, Andersson L, et al. Regulation of vascular endothelial barrier function by Epac, a cAMP-activated exchange factor for Rap GTPase. Blood. 2005; 105:1950–5. [PubMed: 15374886]

16. Yuan Y, Huang Q, Wu HM. Myosin light chain phosphorylation: modulation of basal and agonist-stimulated venular permeability. Am J Physiol. 1997; 272:H1437–43. [PubMed: 9087622]

17. Qiao J, Huang F, Lum H. PKA inhibits RhoA activation: a protection mechanism against endothelial barrier dysfunction. Am J Physiol Lung Cell Mol Physiol. 2003; 284:L972–80. [PubMed: 12588708]

18. Verin AD, Gilbert-McClain LI, Patterson CE, et al. Biochemical regulation of the nonmuscle myosin light chain kinase isoform in bovine endothelium. Am J Respir Cell Mol Biol. 1998; 19:767–76. [PubMed: 9806741]

19. Birukova AA, Liu F, Garcia JG, et al. Protein kinase A attenuates endothelial cell barrier dysfunction induced by microtubule disassembly. Am J Physiol Lung Cell Mol Physiol. 2004; 287:L86–93. [PubMed: 15003930]

20. Boettner B, Van Aelst L. Control of cell adhesion dynamics by Rap1 signaling. Curr Opin Cell Biol. 2009; 21:684–93. [PubMed: 19615876]

21. Takai Y, Ikeda W, Ogita H, et al. The immunoglobulin-like cell adhesion molecule nectin and its associated protein afadin. Annu Rev Cell Dev Biol. 2008; 24:309–42. [PubMed: 18593353]

22. Sayner SL, Alexeyev M, Dessauer CW, et al. Soluble adenylyl cyclase reveals the significance of cAMP compartmentation on pulmonary microvascular endothelial cell barrier. Circ Res. 2006; 98:675–81. [PubMed: 16469954]

23. Sayner SL. Emerging themes of cAMP regulation of the pulmonary endothelial barrier. Am J Physiol Lung Cell Mol Physiol. 2011; 300:L667–78. [PubMed: 21335524]

24. Fukuyama T, Ogita H, Kawakatsu T, et al. Involvement of the c-Src-Crk-C3GRap1 signaling in the nectin-induced activation of Cdc42 and formation of adherens junctions. J Biol Chem. 2005; 280:815–25. [PubMed: 15504743]

25. Sato T, Fujita N, Yamada A, et al. Regulation of the assembly and adhesion activity of E-cadherin by nectin and afadin for the formation of adherens junctions in Madin-Darby canine kidney cells. J Biol Chem. 2006; 281:5288–99. [PubMed: 16361708]

26. Birukova AA, Fu P, Wu T, et al. Afadin controls p120-catenin-ZO-1 interactions leading to endothelial barrier enhancement by oxidized phospholipids. J Cell Physiol. 2012; 227:1883–90. [PubMed: 21732359]

27. Arthur WT, Quilliam LA, Cooper JA. Rap1 promotes cell spreading by localizing Rac guanine nucleotide exchange factors. J Cell Biol. 2004; 167:111–22. [PubMed: 15479739]

28. Birukova AA, Adyshev D, Gorshkov B, et al. GEF-H1 is involved in agonist-induced human pulmonary endothelial barrier dysfunction. Am J Physiol Lung Cell Mol Physiol. 2006; 290:L540–8. [PubMed: 16257999]

29. Birukova AA, Birukov KG, Smurova K, et al. Novel role of microtubules in thrombin-induced endothelial barrier dysfunction. FASEB J. 2004; 18:1879–90. [PubMed: 15576491]

30. Meliton AY, Munoz NM, Meliton LN, et al. Cytosolic group IVa phospholipase A2 mediates IL-8/ CXCL8-induced transmigration of human polymorphonuclear leukocytes in vitro. Journal of inflammation (London, England). 2010; 7:14.

31. Meliton AY, Munoz NM, Zhu X, et al. Attenuated translocation of group IVa phospholipase A2 and up-regulated annexin-1 synthesis by glucocorticoid blocks beta 2-integrin adhesion in neutrophils. J Leukoc Biol. 2008; 83:344–51. [PubMed: 17971499]

32. Birukova AA, Tian X, Tian Y, et al. Rap-afadin axis in control of Rho signaling and endothelial barrier recovery. Mol Biol Cell. 2013; 24:2678–88. [PubMed: 23864716]

33. Singleton PA, Chatchavalvanich S, Fu P, et al. Akt-mediated transactivation of the S1P1 receptor in caveolin-enriched microdomains regulates endothelial barrier enhancement by oxidized phospholipids. Circ Res. 2009; 104:978–86. [PubMed: 19286607]

34. Birukova AA, Fu P, Xing J, et al. Mechanotransduction by GEF-H1 as a novel mechanism of ventilator-induced vascular endothelial permeability. Am J Physiol Lung Cell Mol Physiol. 2010; 298:L837–48. [PubMed: 20348280]

35. Birukova AA, Smurova K, Birukov KG, et al. Microtubule disassembly induces cytoskeletal remodeling and lung vascular barrier dysfunction: Role of Rho-dependent mechanisms. J Cell Physiol. 2004; 201:55–70. [PubMed: 15281089]

36. Birukov KG, Jacobson JR, Flores AA, et al. Magnitude-dependent regulation of pulmonary endothelial cell barrier function by cyclic stretch. Am J Physiol Lung Cell Mol Physiol. 2003; 285:L785–97. [PubMed: 12639843]

37. Birukov KG, Bochkov VN, Birukova AA, et al. Epoxycyclopentenone-containing oxidized phospholipids restore endothelial barrier function via Cdc42 and Rac. Circ Res. 2004; 95:892–901. [PubMed: 15472119]

38. Yan J, Li F, Ingram DA, et al. Rap1a is a key regulator of fibroblast growth factor 2-induced angiogenesis and together with Rap1b controls human endothelial cell functions. Mol Cell Biol. 2008; 28:5803–10. [PubMed: 18625726]

39. Duchniewicz M, Zemojtel T, Kolanczyk M, et al. Rap1A-deficient T and B cells show impaired integrin-mediated cell adhesion. Mol Cell Biol. 2006; 26:643–53. [PubMed: 16382154]

40. Fu P, Birukova AA, Xing J, et al. Amifostine reduces lung vascular permeability via suppression of inflammatory signalling. Eur Respir J. 2009; 33:612–24. [PubMed: 19010997]

41. Moitra J, Sammani S, Garcia JG. Re-evaluation of Evans Blue dye as a marker of albumin clearance in murine models of acute lung injury. Transl Res. 2007; 150:253–65. [PubMed: 17900513]

42. Nonas S, Birukova AA, Fu P, et al. Oxidized phospholipids reduce ventilator-induced vascular leak and inflammation in vivo. Crit Care. 2008; 12:R27. [PubMed: 18304335]

43. Potter MD, Barbero S, Cheresh DA. Tyrosine phosphorylation of VE-cadherin prevents binding of p120- and beta-catenin and maintains the cellular mesenchymal state. J Biol Chem. 2005; 280:31906–12. [PubMed: 16027153]

44. Dejana E, Orsenigo F, Lampugnani MG. The role of adherens junctions and VE-cadherin in the control of vascular permeability. J Cell Sci. 2008; 121:2115–22. [PubMed: 18565824]

45. Takai Y, Nakanishi H. Nectin and afadin: novel organizers of intercellular junctions. J Cell Sci. 2003; 116:17–27. [PubMed: 12456712]

46. Ogita H, Rikitake Y, Miyoshi J, et al. Cell adhesion molecules nectins and associating proteins: Implications for physiology and pathology. Proceedings of the Japan Academy. 2010; 86:621–9. [PubMed: 20551598]

47. Lakshmikanthan S, Sobczak M, Chun C, et al. Rap1 promotes VEGFR2 activation and angiogenesis by a mechanism involving integrin alphavbeta(3). Blood. 2011; 118:2015–26. [PubMed: 21636859]

48. Pannekoek WJ, van Dijk JJ, Chan OY, et al. Epac1 and PDZ-GEF cooperate in Rap1 mediated endothelial junction control. Cell Signal. 2011

49. Wittchen ES, Aghajanian A, Burridge K. Isoform-specific differences between Rap1A and Rap1B GTPases in the formation of endothelial cell junctions. Small GTPases. 2011; 2:65–76. [PubMed: 21776404]

50. Su CF, Liu DD, Kao SJ, et al. Nicotinamide abrogates acute lung injury caused by ischaemia/reperfusion. Eur Respir J. 2007; 30:199–204. [PubMed: 17504797]

51. Shields CJ, Delaney CP, Winter DC, et al. Induction of nitric oxide synthase is a key determinant of progression to pulmonary injury in experimental pancreatitis. Surgical infections. 2006; 7:501–11. [PubMed: 17233567]

52. Kim KS, Suh GJ, Kwon WY, et al. Antioxidant effects of selenium on lung injury in paraquat intoxicated rats. Clinical toxicology (Philadelphia, Pa. 2012; 50:749–53.

53. Lu YC, Yeh WC, Ohashi PS. LPS/TLR4 signal transduction pathway. Cytokine. 2008; 42:145–51. [PubMed: 18304834]

54. Matoba K, Kawanami D, Ishizawa S, et al. Rho-kinase mediates TNF-alpha-induced MCP-1 expression via p38 MAPK signaling pathway in mesangial cells. Biochem Biophys Res Commun. 2010; 402:725–30. [PubMed: 20977889]

55. Nwariaku FE, Rothenbach P, Liu Z, et al. Rho inhibition decreases TNF-induced endothelial MAPK activation and monolayer permeability. J Appl Physiol. 2003; 95:1889–95. [PubMed: 12844496]

56. Xiaolu D, Jing P, Fang H, et al. Role of p115RhoGEF in lipopolysaccharide-induced mouse brain microvascular endothelial barrier dysfunction. Brain Res. 2011; 1387:1–7. [PubMed: 21354111]

57. Guo F, Zhou Z, Dou Y, et al. GEF-H1/RhoA signalling pathway mediates lipopolysaccharide-induced intercellular adhesion molecular-1 expression in endothelial cells via activation of p38 and NF-kappaB. Cytokine. 2012; 57:417–28. [PubMed: 22226621]

58. Xing J, Birukova AA. ANP attenuates inflammatory signaling and Rho pathway of lung endothelial permeability induced by LPS and TNFalpha. Microvasc Res. 2010; 79:26–62.

59. Kratzer E, Tian Y, Sarich N, et al. Oxidative stress contributes to lung injury and barrier dysfunction via microtubule destabilization. Am J Respir Cell Mol Biol. 2012; 47:688–97. [PubMed: 22842495]

60. Mambetsariev I, Tian Y, Wu T, et al. Stiffness-activated GEF-H1 expression exacerbates LPS-induced lung inflammation. PLoS One. 2014; 9:e92670. [PubMed: 24739883]

61. Sans E, Delachanal E, Duperray A. Analysis of the roles of ICAM-1 in neutrophil transmigration using a reconstituted mammalian cell expression model: implication of ICAM-1 cytoplasmic domain and Rho-dependent signaling pathway. J Immunol. 2001; 166:544–51. [PubMed: 11123335]

62. Allingham MJ, van Buul JD, Burridge K. ICAM-1-mediated, Src- and Pyk2-dependent vascular endothelial cadherin tyrosine phosphorylation is required for leukocyte transendothelial migration. J Immunol. 2007; 179:4053–64. [PubMed: 17785844]

63. Turowski P, Martinelli R, Crawford R, et al. Phosphorylation of vascular endothelial cadherin controls lymphocyte emigration. J Cell Sci. 2008; 121:29–37. [PubMed: 18096689]

64. Perez-Moreno M, Davis MA, Wong E, et al. p120-catenin mediates inflammatory responses in the skin. Cell. 2006; 124:631–44. [PubMed: 16469707]

65. Wang YL, Malik AB, Sun Y, et al. Innate immune function of the adherens junction protein p120-catenin in endothelial response to endotoxin. J Immunol. 2011; 186:3180–7. [PubMed: 21278343]

66. Hoshino T, Sakisaka T, Baba T, et al. Regulation of E-cadherin endocytosis by nectin through afadin, Rap1, and p120ctn. J Biol Chem. 2005; 280:24095–103. [PubMed: 15857834]

Highlights

- Activation of Rap1 stimulates barrier restoration during ongoing inflammation

- Rap1 activates afadin and enhances cell junctions during lung barrier recovery

- In parallel, Rap1-afadin complex inhibits NFkB and p38 inflammatory signaling

- These effects define dual mechanism of Rap-dependent lung barrier recovery

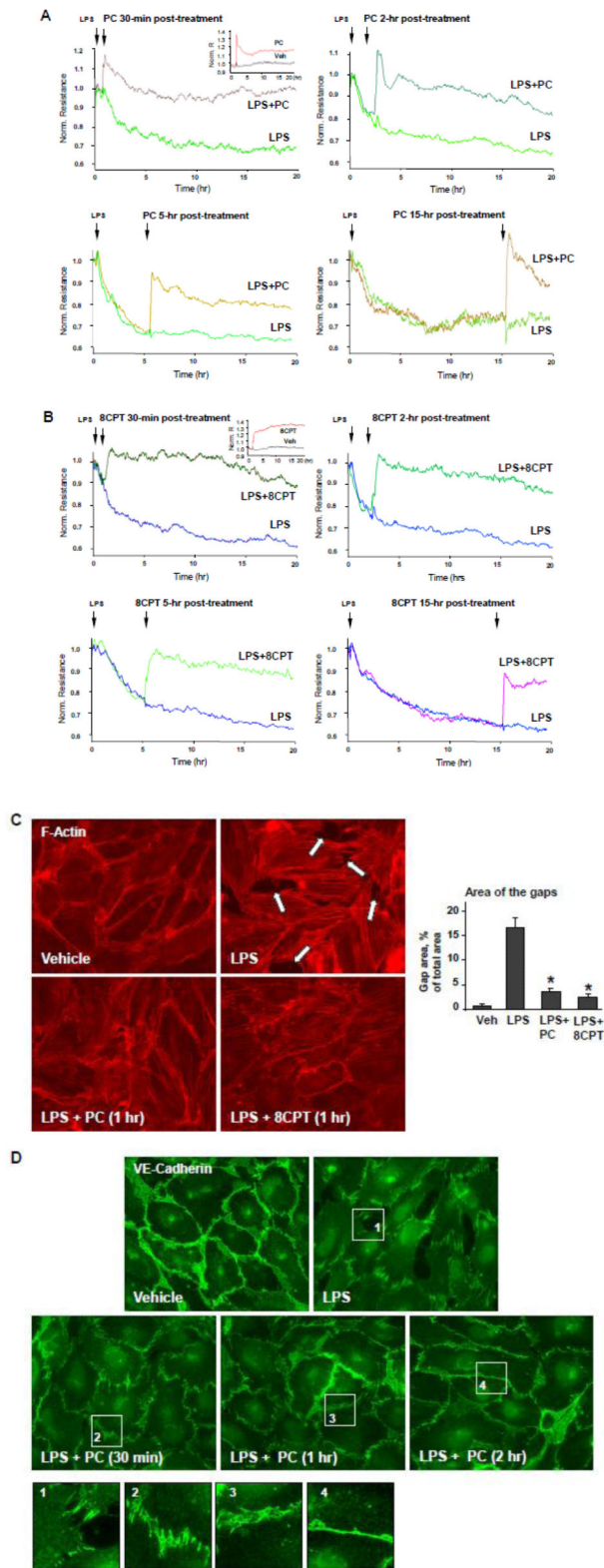- Pharmacologic Rap1activation may reduce lung injury and accelerate ALI recovery

Figure 1. Post-treatment with prostacyclin and 8CPT recovers LPS-induced EC permeability and monolayer disruption

Pulmonary EC plated on microelectrodes were stimulated with LPS (300 ng/ml), followed by: **A** – PC (200 ng/ml); or **B** – 8CPT (50 μM) post-treatment at different time points after LPS challenge, as shown by arrows. Transendothelial resistance reflecting EC monolayer barrier properties was monitored over 20 hours after treatments. Insets in panels A and B show increase in transendothelial resistance caused by treatment with PC or 8CPT alone. **C and D:** Pulmonary EC grown on glass coverslips were challenged with LPS for 5 hrs, followed by PC or 8CPT treatment for additional 30 min, 1 hr, or 2 hrs, as indicated. **C** – Analysis of actin cytoskeletal rearrangement was performed by immunofluorescence staining with Texas Red phalloidin. Paracellular gaps are marked by arrows. Bar graph represents quantitative analysis of paracellular gap formation in control and treated HPAEC. Data are expressed as mean + SD of four independent experiments; *p<0.05, vs. LPS alone. **D** – Immunofluorescence staining for VE-cadherin was performed to visualize adherens junctions. Insets below depict higher magnification images of VE-cadherin patterns in cell junction areas after different treatments.
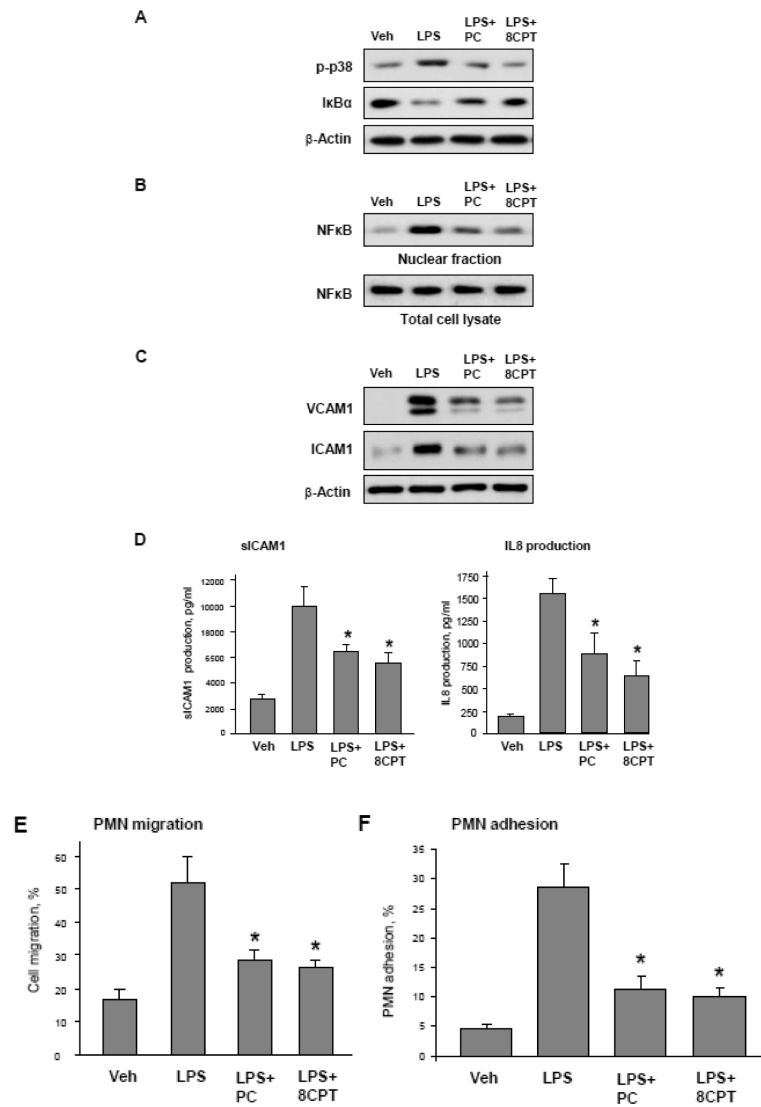
Figure 2. PC and 8CPT post-treatment attenuates LPS-induced EC inflammation
Pulmonary EC were challenged with LPS followed by post-treatment with PC or 8CPT. **A** –
PC or 8CPT post-treatment 30 min after LPS addition followed by 2-hr incubation.
Phosphorylation of p38 MAP kinase and degradation of IκBα was detected by
immunoblotting with corresponding antibodies. Equal protein loading was verified by
membrane probing with β-actin antibody. **B** – PC or 8CPT post-treatment 30 min after LPS
addition followed by 2-hr incubation. NFκB nuclear translocation was assessed by
fractionation assay. Content of NFκB in corresponding total cell lysates was analyzed to
ensure equal loading. **C** – PC or 8CPT post-treatment 5 hrs after LPS addition followed by
19-hr incubation. Protein expression of VCAM1 and ICAM1 in stimulated EC was detected
by immunoblotting. Equal protein loading was verified by membrane probing with β-actin
antibody. **D** – PC or 8CPT post-treatment 5 hrs after LPS addition followed by 19-hr
incubation. Secretion of soluble ICAM1 and IL-8 was evaluated by ELISA assay. **E and F:**
PC or 8CPT post-treatment 5 hrs after LPS addition followed by 19-hr incubation. **E** –
Analysis of PMN migration stimulated by preconditioned medium from EC activated by

LPS with or without PC or 8CPT post-treatment. **F** – Analysis of PMN adhesion to EC activated by LPS with or without PC or 8CPT post-treatment. Data are expressed as mean + SD of four independent experiments; *p<0.05, vs. LPS alone.
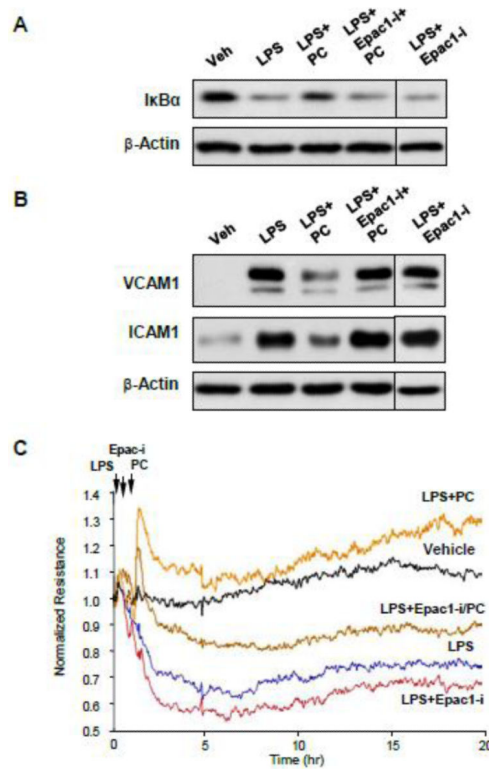
Figure 3. Epac inhibitor abolishes protective effects of PC and 8CPT post-treatment on LPS-induced EC inflammation and hyperpermeability

Pulmonary EC were challenged with LPS followed by post-treatment with vehicle or PC with or without Epac inhibitor (50 μM). **A** – PC and Epac inhibitor were added 30 min after LPS challenge and cells were incubated for additional 2 hrs. IκBα degradation was evaluated by immunoblotting of total cell lysates. **B** – PC and Epac inhibitor were added 5 hrs after LPS challenge and cells were incubated for additional 19 hrs. Expression of ICAM1 and VCAM1 was detected by immunoblotting with corresponding antibodies. Equal protein loading was verified by probing with β-actin antibody. **C** – Pulmonary EC were challenged with LPS with or without post-treatment with PC, with or without Epac inhibitor at the times indicated by arrows, and TER was measured over 20 hrs.
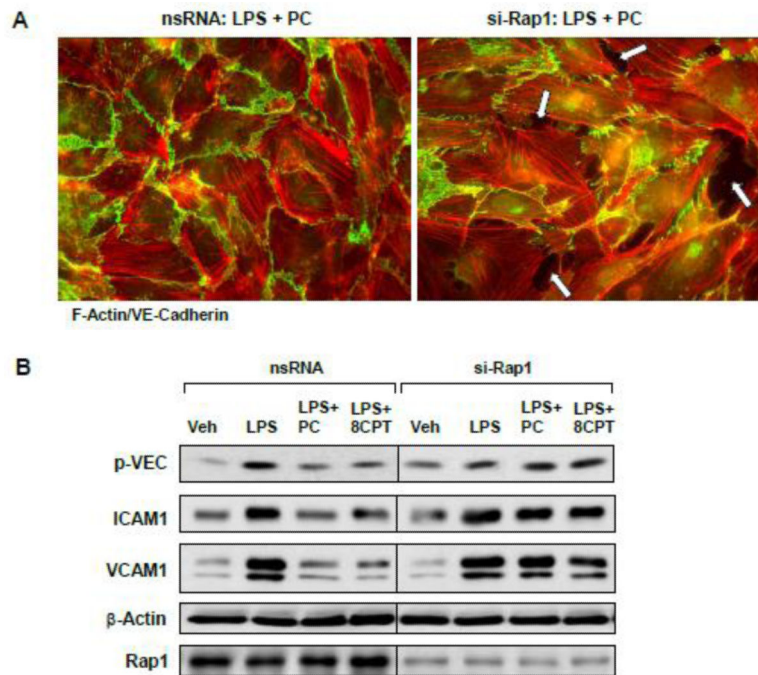
Figure 4. Rap1 knockdown attenuates PC-induced EC monolayer recovery and attenuation of inflammation caused by LPS

A – EC plated on coverslips were transfected with Rap1-specific siRNA or non-specific RNA 48 hrs prior to LPS treatment followed by PC post-treatment (5 hrs after LPS) and additional 1-hr incubation. Cytoskeletal remodeling was assessed by immunofluorescence staining for F-actin with Texas Red phalloidin. VE-cadherin was detected by staining with VE-cadherin antibody. Shown are merged images of F-actin (red) and VE-cadherin (green) staining. Arrows indicate intercellular gaps. Results are representative of three independent experiments. **B** – EC were transfected with Rap1-specific siRNA or non-specific RNA 48 hrs prior to LPS treatment followed by PC or 8CPT post-treatment (5 hrs after LPS) and additional 19-hr incubation. VE-cadherin phosphorylation and expression of ICAM1 and VCAM1 was detected by immunoblotting with corresponding antibodies. Equal protein loading was verified by membrane probing with β-actin antibody. Depletion of Rap1 was confirmed by membrane probing with Rap1 antibody.
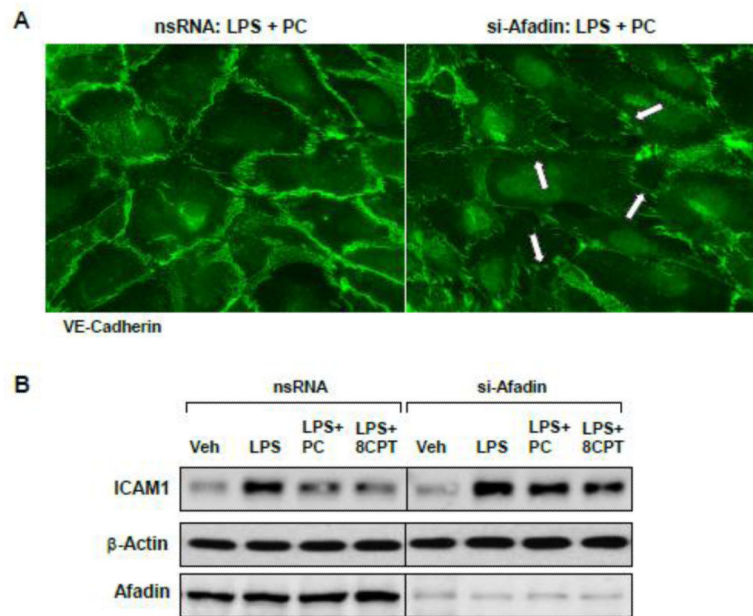
Figure 5. Afadin knockdown attenuates protective effects of PC post-treatment on EC monolayer recovery and attenuation of inflammation caused by LPS

A – EC plated on coverslips were transfected with afadin-specific siRNA or non-specific RNA 72 hrs prior to LPS treatment followed by PC post-treatment (5 hrs after LPS) and additional 1-hr incubation. VE-cadherin was detected by staining with VE-cadherin antibody. Arrows show sites of VE-cadherin disappearance from cell junctions. Results are representative of three independent experiments. **B** – EC were transfected with afadin-specific siRNA or non-specific RNA 72 hrs prior to LPS treatment followed by PC or 8CPT post-treatment (5 hrs after LPS) and additional 19-hr incubation. Expression of ICAM1 and VCAM1 in control and afadin-depleted EC was detected by immunoblotting with corresponding antibodies. Equal protein loading was verified by membrane probing with β-actin antibody. Depletion of afadin was confirmed by membrane probing with afadin antibody.
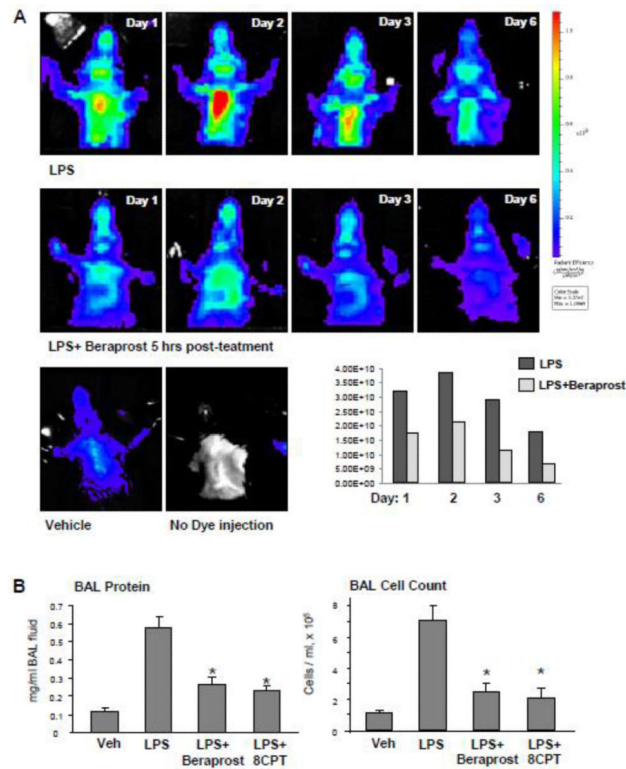
Figure 6. Post-treatment with beraprost attenuates LPS-induced lung injury and barrier dysfunction

A – Live imaging analysis of lung vascular barrier dysfunction after LPS intratracheal injection with and without beraprost post treatment (i.v., 5 hrs after LPS). LPS-induced accumulation of fluorescent Angiosense 680 EX imaging agent in the lungs of same animals was detected by Xenogen IVIS 200 Spectrum imaging system after 1, 2, 3 and 6 days after LPS challenge as described in Methods and presented in arbitrary colors. Bar graph represents quantitative analysis of imaging data. **B** - Beraprost or 8CPT injection (i.v.) was performed 5 hrs after LPS administration (i.t.). After 24 hrs of LPS challenge mice were sacrificed, BAL collection was performed, and measurements of protein concentration and total cell count were performed in BAL samples obtained from control and experimental groups. Data are expressed as mean + SD of four independent experiments; n=6-10 per condition; *p<0.05 vs. LPS alone.
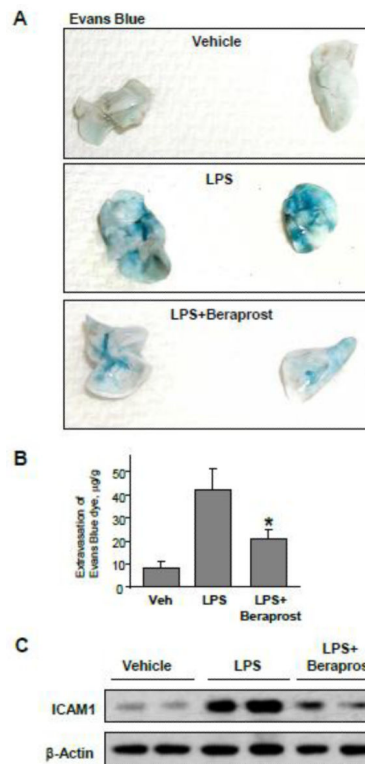
Figure 7. Post-treatment with beraprost attenuates LPS-induced lung vascular leak and inflammation

Beraprost injection (i.v.) was performed 5 hrs after i.t. LPS administration. The experiment was terminated after 24 hrs of LPS challenge. **A** – Evans blue dye (30 ml/kg, i/v) was injected 2 hr before termination of the experiment. Photographs depict lung vascular permeability was assessed by Evans blue accumulation in the lung tissue. **B** – Quantitative analysis of Evans blue labeled albumin extravasation was performed by spectrophotometric analysis of Evans blue extracted from the lung tissue samples; n=4 per condition; *p<0.05. **C** – Protein expression of ICAM-1 in control and treated lung tissue samples was evaluated by immunoblotting. Equal protein loading in western blot experiments was confirmed by determination of β-actin content in tissue samples.
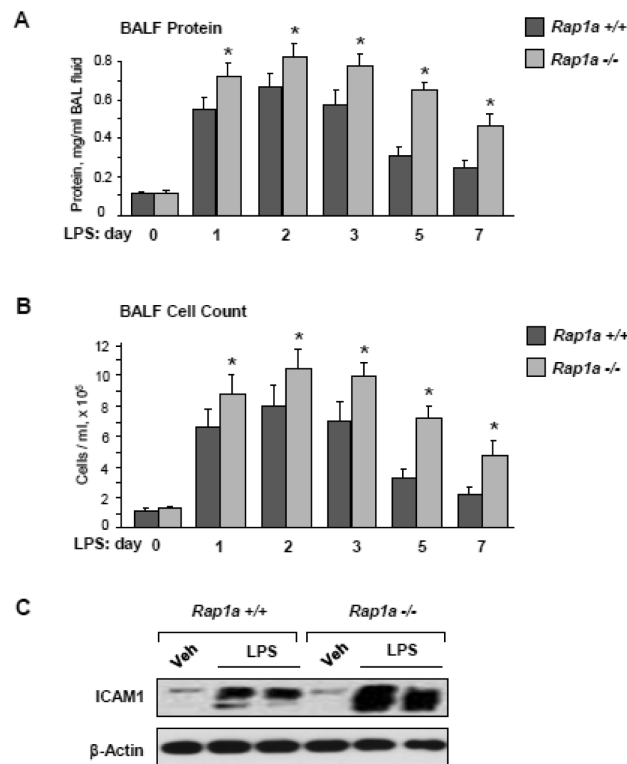
Figure 8. Delayed lung recovery in LPS-challenged *Rap1a−/−* mice

BAL protein content (**A**) and cell count (**B**) was determined in control and Rap1a−/−mice after 1, 2, 3, 5 and 7 days of LPS challenge Data are expressed as mean + SD of four independent measurements; *p<0.05 vs. *Rap1+/+* mice. **C** – ICAM1 protein expression in control and *Rap1a−/−* lung tissue samples was evaluated by immunoblotting. Equal protein loading in western blot experiments was confirmed by determination of β-actin content in tissue samples.
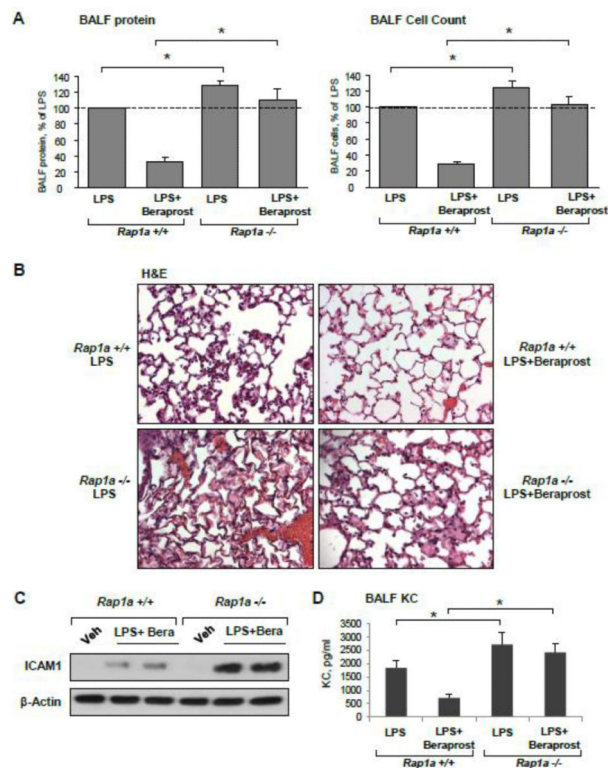
Figure 9. Attenuation of protective effects of beraprost post-treatment in *Rap−/−* mice
Beraprost injection (i.v.) of *Rap1−/−* mice and matched wild type controls was performed 5 hrs after i.t. LPS administration. The experiment was terminated after 24 hrs of LPS challenge. **A** - BAL protein content and cell count measurements. **B** – Histological analysis of lung tissue by hematoxilin & eosin staining (x40 magnification). **C** – ICAM1 protein expression in control and treated lung tissue samples was evaluated by immunoblotting. Equal protein loading in western blot experiments was confirmed by determination of β-actin content in tissue samples. **D** – The levels of the mouse KC were measured in BAL samples using ELISA assay. Data are expressed as mean + SD of four independent experiments; *p<0.05.